Constraining the neutron-proton effective mass splitting in neutron-rich matter

Bao-An Li*
Department of Physics, Arkansas State University, State University, Arkansas 72467-0419
(Received 19 February 2004; published 3 June 2004)

Within Bombaci's phenomenological single-nucleon potential model we study the neutron-proton effective mass splitting m_n^*-m_p^* in neutron-rich matter. It is shown that an effective mass splitting of $m_n^* < m_p^*$ leads to a symmetry potential that is inconsistent with the energy dependence of the Lane potential constrained by the nucleon-nucleus scattering experimental data.

DOI: 10.1103/PhysRevC.69.064602 PACS number(s): 25.70.−z, 14.20.Dh, 21.65.+f

One of the most fundamental properties characterizing the propagation of a nucleon in nuclear medium is its effective mass [1–3]. The latter describes to leading order the effects related to the nonlocality of the underlying nuclear effective interactions and the Pauli exchange effects in many-fermion systems. In neutron-rich matter, an interesting new question arises as to whether the effective mass m_n^* for neutrons is higher or lower than that for protons m_p^*. Microscopic many-body theories, e.g., the Landau-Fermi liquid theory [4] and the Brueckner-Hartree-Fock (BHF) approach [5], predict that $m_n^* > m_p^*$ in neutron-rich matter. On the other hand, some effective interactions within phenomenological approaches predict the opposite [6]. Unfortunately, up to now almost nothing is known experimentally about the neutron-proton effective mass splitting m_n^*-m_p^* in neutron-rich medium. Knowledge about nucleon effective mass in neutron-rich matter is critically important for understanding several properties of neutron stars [7–9]. It is also important for the reaction dynamics of nuclear collisions induced by radioactive nuclei, such as, the degree and speed of isospin diffusion, the neutron-proton differential collective flow as well as the isospin equilibrium [6,10–12]. Moreover, it influences the magnitude of shell effects and basic properties of nuclei fare from stability [1]. However, even the sign of the neutron-proton effective mass splitting remains rather controversial theoretically. It is thus imperative to constrain the neutron-proton effective mass splitting in neutron-rich matter using experimental data. In a recent study by Rizzo *et al.* [6], nuclear reactions with radioactive beams were proposed as a means to disentangle the sign of the neutron-proton effective mass splitting in neutron-rich matter. In this note we take a completely different approach for the same purpose. We show that an effective mass splitting of $m_n^* < m_p^*$ leads to a symmetry potential that is inconsistent with the energy dependence of the Lane potential constrained by existing nucleon-nucleus scattering data. The effective mass splitting of $m_n^* < m_p^*$ is thus ruled out phenomenologically using experimental data indirectly.

The effective mass m_τ^* of a nucleon τ (n or p) is determined by the momentum-dependent single nucleon potential U_τ via [3]

$$\frac{m_\tau^*}{m_\tau} = \left\{ 1 + \frac{m_\tau}{\hbar^2 k}\frac{dU_\tau}{dk} \right\}^{-1}_{k=k_\tau^F}, \tag{1}$$

where k_τ^F is the nucleon Fermi wave number in asymmetric nuclear matter of isospin asymmetry $\delta \equiv (\rho_n - \rho_p)/\rho$ with ρ, ρ_n, and ρ_p being the nucleon, neutron, and proton density, respectively. The effective mass defined in Eq. (1) is the so-called k mass which is identical to the total effective mass when the single nucleon potential is energy independent [2,3]. For the single nucleon potential U_τ, following Rizzo *et al.* [6] we use the phenomenological formalism of Bombaci [13]:

$$\begin{aligned} U_\tau(k,u,\delta) &= Au + Bu^\sigma - \frac{2}{3}(\sigma-1)\frac{B}{\sigma+1}\left(\frac{1}{2}+x_3\right)u^\sigma\delta^2 \\ &\pm\left[-\frac{2}{3}A\left(\frac{1}{2}+x_0\right)u - \frac{4}{3}\frac{B}{\sigma+1}\left(\frac{1}{2}+x_3\right)u^\sigma\right]\delta \\ &+ \frac{4}{5\rho}\left[\frac{1}{2}(3C-4z_1)\mathcal{I}_\tau + (C+2z_1)\mathcal{I}_{\tau'}\right] \\ &+ \left(C \pm \frac{C-8z_1}{5}\delta\right)u\cdot g(k), \end{aligned} \tag{2}$$

where $u \equiv \rho/\rho_0$ is the reduced density and $\pm$ is for neutrons/protons. In the earlier $\mathcal{I}_\tau = [2/(2\pi)^3]\int d^3k f_\tau(k) g(k)$, $g(k)$ is a momentum regulator $g(k) \equiv 1/[1+(k/\Lambda)^2]$, and $f_\tau(k)$ is the phase space distribution function. The parameter $\Lambda = 1.5K_F^0$ where K_F^0 is the nucleon Fermi wave number in symmetric nuclear matter at normal density ρ_0. With $A = -144$ MeV, $B = 203.3$ MeV, $C = -75$ MeV, and $\sigma = 7/6$ the Bombaci formalism reproduces all ground state properties including an incompressibility of $K_0 = 210$ MeV of symmetric nuclear matter [6,13]. It should be noticed that the Bombaci expression is an extension of the well known Gale-Bertsch-Das Gupta formalism [14] from symmetric to asymmetric nuclear matter. The various terms are motivated by the HF analysis using the Gogny effective interaction [15,16]. This potential depends explicitly on the momentum but not the total energy of nucleons. Thus, the k-mass obtained is the same as the total effective mass. One should also mention that only the last term is momentum dependent. Thus, the Λ parameter sets the scale of the momentum dependence of the nucleon potential U_τ and also the scale of the effective mass. The

*Email address: bali@astate.edu

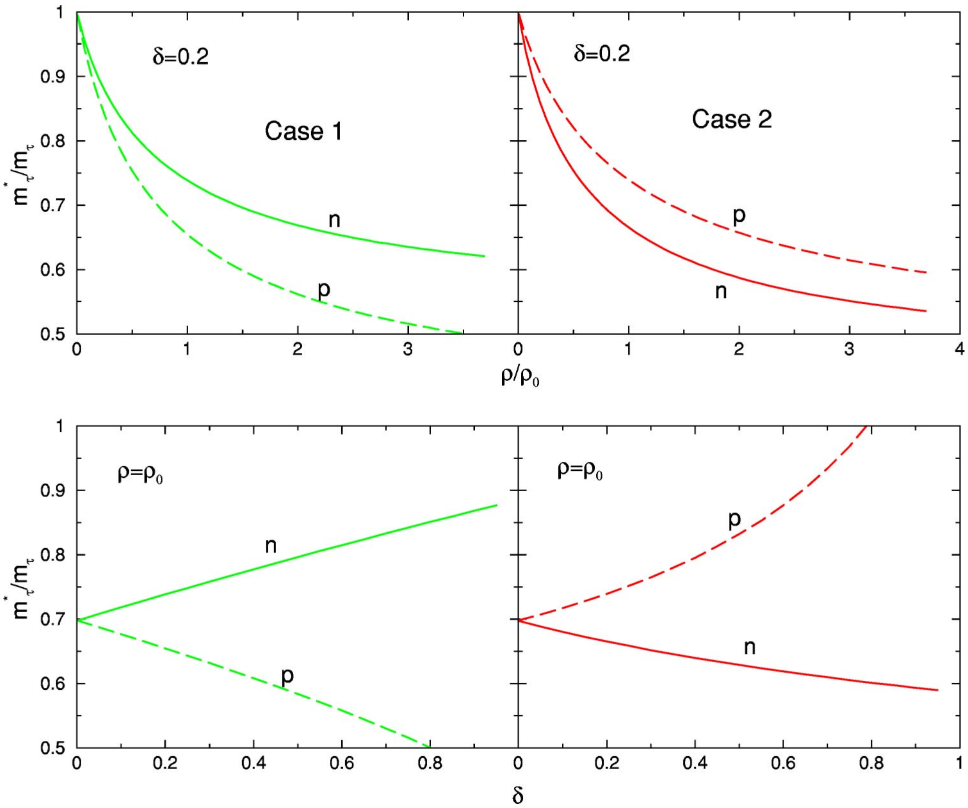

FIG. 1. (Color online) Nucleon effective masses as a function of density (upper window) and isospin asymmetry (lower window) with the two parameter sets.

value of Λ parameter was determined by the ground state properties of symmetric nuclear matter. It can also appropriately reproduce the momentum dependence of the empirical isoscalar nuclear optical potential as we shall show in the following. The expressions in Eq. (2) lead to an effective mass [6,13]:

$$\frac{m_\tau^*}{m_\tau} = \left\{ 1 + \frac{-\dfrac{2m_\tau}{\hbar^2}\dfrac{1}{\Lambda^2}\left(C \pm \dfrac{C-8z_1}{5}\delta\right)u}{\left[1+\left(\dfrac{k_{F0}}{\Lambda}\right)^2(1\pm\delta)^{2/3}u^{2/3}\right]^2} \right\}^{-1}. \tag{3}$$

It is noticed that the $(1\pm\delta)^{2/3}u^{2/3}$ term comes from the nucleon Fermi wave number k_τ^F squared, and $\pm$ is for $\tau = n/p$. The three parameters x_0, x_3, and z_1 can be adjusted to mimic different predictions on the density-dependent symmetry energy and the neutron-proton effective mass splitting. Two sets of parameters can be chosen to give two opposite nucleon effective mass splittings, but almost the same symmetry energy $E_{\text{sym}}(\rho)$ [6]. The parameter set $z_1 = -36.75$ MeV, $x_0 = -1.477$, and $x_3 = -1.01$ (case 1) leads to $m_n^* > m_p^*$ while the one with $z_1 = 50$ MeV, $x_0 = 1.589$, and $x_3 = -0.195$ (case 2) leads to $m_n^* < m_p^*$ at all nonzero densities and isospin asymmetries. Shown in Fig. 1 are the nucleon effective masses as functions of density and isospin asymmetry in both cases. It is seen that the neutron-proton effective mass splittings, opposite in signs, increase in magnitudes in both cases with the density and isospin asymmetry. Thus, large magnitides of effective mass splittings can be obtained in dense neutron-rich matter.

These two sets of parameters were shown to lead to rather different results for several observables in heavy-ion reactions induced by neutron-rich nuclei [6].

Our analysis is based on the consideration that both the isoscalar and isovector parts of the single nucleon potential must have asymptotic values at ρ_0 in agreement with the real parts of the corresponding nucleon optical potentials constrained by nucleon-nucleus scattering experiments. We first examine the isoscalar potentials with the two sets of parameters. The quantity $(U_n + U_p)/2$ is a good approximation of the isoscalar potential since the δ^2 in Eq. (2) is negligibly small. It is now customary and a more stringent test of the isoscalar potentials to compare them with the variational many-body (VMB) predictions by Wiringa [15,17–19]. In the VMB theory the single nucleon potential was obtained by using a realistic Hamiltonian that fits nucleon-nucleon scattering data, few-body nuclear binding energies and nuclear matter saturation properties. It also reproduces the experimental nucleon optical potential available mainly at low energies [20]. Shown in Fig. 2 is a comparison of isoscalar potentials using Eq. (2) with the VMB predictions using the *UV*14 two-body potential and the *UVII* three-body potential [17]. First of all, the isoscalar potentials are almost independent of the neutron-proton effective mass splittings as one expects. In both cases the isoscalar potentials using Eq. (2) are in good agreement with the VMB predictions up to about $k = 2.5$ fm^{-1}. At higher momenta where combinations of different two-body and three-body forces lead to somewhat different predictions especially at high densities [17], the Bombaci formalism leads to slightly lower values. Nevertheless, the quality of agreement with the VMB predictions found here is compatible with those using all other models [15,18].

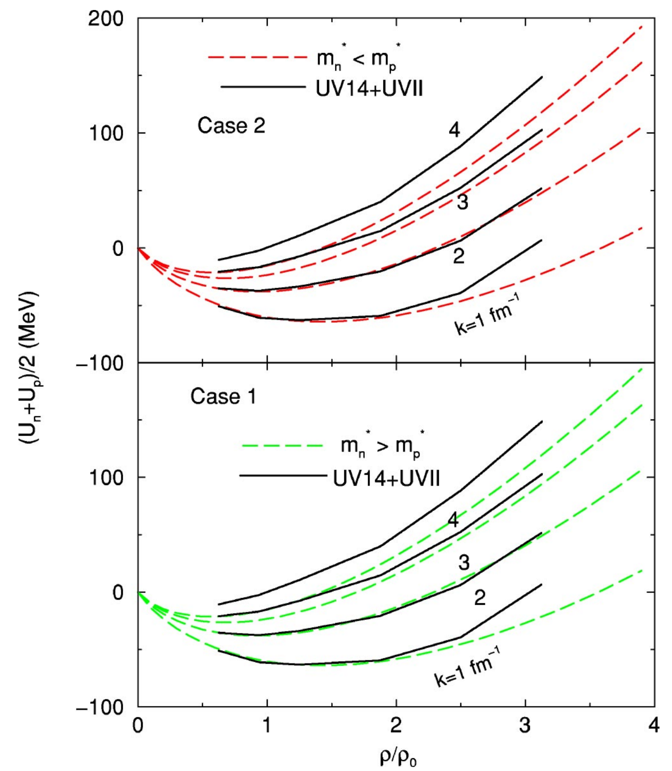

FIG. 2. (Color online) Strengths of the isoscalar potential as a function of density at the four wave numbers for case 1 (lower window) and case 2 (upper window) in comparison with the variational many-body calculations.

We now turn to the isovector part of the nucleon potential in both cases. The strength of the isovector nucleon optical potential, i.e., the symmetry or Lane potential [21], can be extracted from $U_{\rm Lane} \equiv (U_n - U_p)/2\delta$ at ρ_0. Systematic analyses of a large number of nucleon-nucleus scattering experiments at beam energies below about 100 MeV [22] indicates undoubtedly that the Lane potential decreases approximately linearly with increasing beam energy $E_{\rm kin}$, i.e.:

$$U_{\rm Lane} = a - bE_{\rm kin}, \tag{4}$$

where $a \simeq 22-34$ MeV and $b \simeq 0.1-0.2$ [23,24].

Shown in Fig. 3 are the theoretical symmetry potentials in the two cases in comparison with the Lane potential constrained by the experimental data. The vertical bars are used to indicate the uncertainties of the coefficients a and b in Eq. (4). It is seen that with the effective mass splitting $m_n^* > m_p^*$ (case 1) the strength of the symmetry potential decreases with increasing energy. This trend is in agreement with the experimental indication. Moreover, the slope of the calculated symmetry potential with respect to energy is about right although the magnitude obtained is slightly higher. Since it is not the purpose of this work to find the best parameter set to reproduce the empirical Lane potential, no attempt is made to readjust any of the parameters first proposed in Refs. [6,13]. In case 2, however, the most striking feature is that the symmetry potential increases with the increasing beam energy. This is in stark contrast with the experimental indications. The characteristically wrong energy dependence of

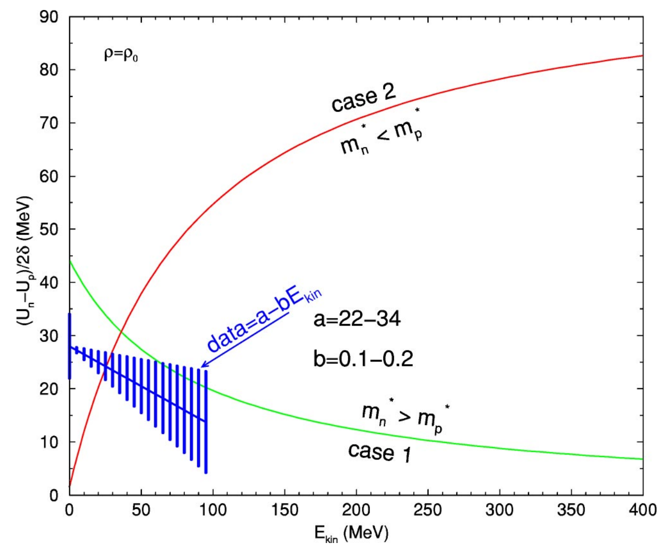

FIG. 3. (Color online) Strength of the isovector potential at normal density ρ_0 as a function of nucleon kinetic energy.

the symmetry potential in this case thus excludes definitely the neutron-proton effective mass splitting of $m_n^* < m_p^*$ in neutron-rich matter.

Our finding here is consistent with that of the earlier work by Sjöberg in the framework of the Landau-Fermi liquid theory [4], BHF predictions [5] as well as Hartree-Fock calculations using the Gogny effective interaction [12]. Within the Landau-Fermi liquid theory, very interestingly, the nucleon effective mass splitting has the analytical and physically transparent relation [4]

$$(m_n^* - m_p^*)/m = \frac{m_n^* k_n}{3\pi^2}[f_1^{\rm nn} + (k_p/k_n)^2 f_1^{\rm np}] - \frac{m_p^* k_p}{3\pi^2}[f_1^{\rm pp} + (k_n/k_p)^2 f_1^{\rm np}], \tag{5}$$

where $f_1^{\rm nn}, f_1^{\rm pp}$, and $f_1^{\rm np}$ are the neutron-neutron, proton-proton, and neutron-proton quasiparticle interactions projected on the $l=1$ Legendre polynomial, as for the effective mass in a one-component Fermi liquid. Microscopic NN interactions predict all f_1's are negative in symmetric matter at nuclear matter density and in asymmetric matter at tree level. It can be seen then that the proton effective mass is smaller in neutron-rich matter due to the coupling of the protons to the denser neutron background, i.e., the term $(k_n/k_p)^2 f_1^{\rm np}$ is dominant in Eq. (5) earlier, leading to $m_n^* > m_p^*$ as shown numerically in Fig. 3 of Ref. [4].

In summary, using the Bombaci phenomenological formalism for single nucleon potentials in isospin asymmetric nuclear matter we analyzed the isoscalar and isovector nucleon optical potentials in comparison with the empirical ones constrained by the experimental data. We found that a neutron-proton effective mass splitting of $m_n^* < m_p^*$ leads to a characteristically wrong energy dependence of the Lane potential. Thus, the possibility of $m_n^* < m_p^*$ in neutron-rich matter is ruled out indirectly by the experimental data.

This research was supported in part by the National Science Foundation under Grant Nos. PHY-0088934 and PHY-0243571.

[1] J. Dobaczewski, Acta Phys. Pol. B **30**, 1647 (1999).
[2] J. W. Negele and K. Yazaki, Phys. Rev. Lett. **62**, 71 (1989).
[3] J. P. Jeukenne, A. Lejeune, and C. Mahaux, Phys. Rep., Phys. Lett. **25C**, 83 (1976).
[4] O. Sjöberg, Nucl. Phys. **A265**, 511 (1976).
[5] I. Bombaci, and U. Lombardo, Phys. Rev. C **44**, 1892 (1991); W. Zuo, I. Bombaci and U. Lombardo, *ibid.* **60**, 24605 (1999); W. Zuo, A. Lejeune, U. Lombardo, and J. F. Mathiot, Eur. Phys. J. A **14**, 469 (2002).
[6] J. Rizzo, M. Colonna, M. DiToro, and V. Greco, Nucl. Phys. **A732**, 202 (2004), and references therein.
[7] H. A. Bethe, Rev. Mod. Phys. **62**, 801 (1990).
[8] J. Cooperstein, Nucl. Phys. **A438**, 722 (1985).
[9] M. Farine *et al.*, Nucl. Phys. **A696**, 396 (2001).
[10] V. R. Pandharipande and S. C. Pieper, Phys. Rev. C **45**, 791 (1992).
[11] D. Persram and C. Gale, Phys. Rev. C **65**, 064611 (2002).
[12] B. A. Li, C. B. Das, S. Das Gupta, and C. Gale, nucl-th/0312054; Nucl. Phys. **A735**, 563 (2004).
[13] I. Bombaci, in *Isospin Physics in Heavy-Ion Collisions at Intermediate Energies*, edited by B. A. Li and W. Udo Schröder (Nova Science, New York, 2001), Chap. 2.
[14] C. Gale *et al.*, Phys. Rev. C **35**, 1666 (1987).
[15] C. Gale *et al.*, Phys. Rev. C **41**, 1545 (1990).
[16] C. B. Das, S. Das Gupta, C. Gale, and B. A. Li, Phys. Rev. C **67**, 034611 (2003).
[17] R. B. Wiringa, Phys. Rev. C **38**, 2967 (1988).
[18] P. Danielewicz and G. F. Bertsch, Nucl. Phys. **A533**, 712 (1991); Q. Pan and P. Danielewicz, Phys. Rev. Lett. **70**, 2062 (1993); P. Danielewicz, Nucl. Phys. **A673**, 375 (2000).
[19] P. Danielewicz, R. Lacey, and W. G. Lynch, Science **298**, 1592 (2002).
[20] L. P. Csernai, G. Fai, C. Gale, and E. Osnes, Phys. Rev. C **46**, 736 (1992).
[21] A. M. Lane, Nucl. Phys. **35**, 676 (1962).
[22] D. M. Patterson *et al.*, Nucl. Phys. **A263**, 261 (1976); J. Rapaport *et al.*, *ibid.* **A313**, 1 (1979); **A330**, 15 (1979); R. P. De Vito *et al.*, Phys. Rev. Lett. **47**, 628 (1981); R. De Leo *et al.*, Phys. Lett. **98B**, 233 (1981); K. Kwiatkowski *et al.*, Nucl. Phys. **A301**, 349 (1978).
[23] J. R. Rook, Nucl. Phys. **A222**, 596 (1973); J. Dabrowski *et al.*, Can. J. Phys. **52**, 1768 (1974); J. P. Jeukenne *et al.*, Phys. Rev. C **10**, 1391 (1974).
[24] P. E. Hodgson, *The Nucleon Optical Model* (World Scientific, Singapore, 1994).